Design and Optical Performance of a Single-Junction GaAs Nanowire-Ge Solar Cell

V. Sudheer Kumar Sistla
Department of Electronics and Communication Engineering, Koneru Lakshmaiah Education Foundation, India
sudheer.ssk39@gmail.com

Surendra Kumar Bitra
Astra Microwave Products Limited, India
bitrasurendrakumar@gmail.com

Santhosh Chella
Department of Electronics and Communication Engineering, Koneru Lakshmaiah Education Foundation, India
csanthosh@kluniversity.in (corresponding author)

Received: 15 June 2023 | Revised: 20 July 2023 | Accepted: 4 August 2023

 DOI: https://doi.org/10.48084/etasr.6121

ABSTRACT

Solar cells are one of the most effective methods available for energy harvesting and are constructed from a variety of materials. In recent years, the use of novel materials for low-cost, high-efficiency photovoltaics has been one of the most exciting breakthroughs. This study conducted an in-depth investigation into the optical characteristics of GaAs nanowires on a Ge bottom cell. Geometric optimization of nanowires is necessary to increase solar cell performance metrics. The absorption efficiency per unit volume was considerably boosted over its traditional bulk and thin-film counterparts as a result of inherent antireflection, intensive stimulation of resonant modes, and optical antenna effects. A 3D FDTD framework was used to acquire optical properties and incorporate numerical values. Under typical AM 1.5G illumination, the diameter of GaAs nanowires was optimized to 170 nm.

Keywords-absorption; E&H field; FDTD; GaAs nanowire; III-V semiconductor nanowires; optical simulation

I. INTRODUCTION

The utilization of solar energy is significant for meeting future energy demands at low cost. In the photovoltaic (PV) market, thin-film technology is gaining great attention due to its simplicity, ease of fabrication, reduced dimensions [1], light weight [2], and reduced cost, among the various types of solar cells. However, the thin-film technology has major disadvantages, such as a reduction in solar conversion efficiency in longer spectral regions due to reduced absorption [1]. To overcome this problem, researchers adopt various strategies to improve efficiency while preserving its advantages. To do so, the amount of light trapping mechanisms is increased by using several dielectric and metallic nanostructures in various dimensions, such as diffractive gratings, textured electrodes, photonic crystals, antireflection coatings, nanoparticles, nanowires (NW), nanofillers, etc. [3].

Of all these different nanostructures, NW-based solar cells are quite popular for improving optical performance in PV devices, as they show improved electrical and optical properties compared to traditional wafer- or thin-film-based solar cells [4]. The ability to capture an enormous amount of light, decrease reflection, fine-tune the band gap, and improve defect tolerance are just a few advantages [4-5]. To realize these NW structures, thin film solar cells are integrated using different materials, such as silicon, II-VI group, III-V group, etc. [6]. Furthermore, because of their direct bandgap structure, high absorption coefficient [7], and strong resistance to high energy rays in space, III-V group semiconducting materials are attracting a lot of attention, particularly for solar space applications [8]. However, gallium-arsenide (GaAs)-based thin-film solar cells showed the highest efficiency, up to 29.1% higher than others, such as III-V materials [9]. Due to the limitations in the efficiency of single-junction solar cells, tandem cells are developed [9].

GaAs nanostructures over germanium (Ge) substrates are one such configuration of two-junction solar cells. Ge provides considerable advantages, such as a perfect match of lattice constant and thermal expansion [11], remarkable strength, and low weight [10], leading to improvements in optical properties and cell efficiency. GaAs solar cells have great radiation resistance and low temperature coefficients to achieve high

conversion efficiency [10]. Since GaAs has a higher optical absorption band, it is well suited for solar energy conversion. Combining GaAs with a Ge bottom cell, which shares the same lattice constant, allows the creation of solar cells [9].

This study focused on the optical modeling of a GaAs single NWs on a Ge cell bottom and a vertical junction. The optimized length and diameter of GaAs NW (L and D) were used to calculate the absorption, transmittance, and reflection characteristics curves for fixed length and pitch in a 0.5 ratio for the highest absorption and cell efficiency. In solar cell design, the D/P ratio is called the Fill Factor, where D is the diameter of the nanowire and P is the highest power output of the solar cell (Pmax). Pmax is the highest amount of electricity that a solar cell can produce under certain conditions. The Pmax value is not a fixed constant, as it can change depending on irradiance (the intensity of light hitting the solar cell), temperature, and the external load connected to the solar cell during testing. Because of this, the Pmax value is specific to how the solar cell works. Different materials have different absorption characteristics and can absorb light more efficiently at certain wavelengths. In general, if a material has an increased absorptance at shorter wavelengths, it means that it is more effective at absorbing light in that range. At shorter wavelengths, the behavior of light can be influenced by factors such as the energy band structure of the material and the electronic transitions that occur. In certain materials or structures, such as thin films or coatings, it is possible to design them to minimize reflection and transmission losses at shorter wavelengths. It is important to note that the specific behavior of materials for absorbance, reflection, and transmission at different wavelengths can vary significantly depending on the material's composition, structure, and other factors. Different materials may exhibit different optical properties, making them more suitable for specific applications.

II. LITERATURE SURVEY

Solar cells are widely used in optoelectronic devices based on their geometry to analyze the effects of size, height, band gap, and PV efficiency with III-V semiconductor nanomaterials such as GaAs NWs [14-15]. Current production conditions have shown that GaAs/inactive-Ge cells can provide a larger area, reduced weight, and high-efficiency cells due to their monolithic tandem [6, 16]. Single NWs are used in the design of solar cells to provide better performance with different geometries [6-7] while introducing a Ge (111) substrate interdiffused with GaAs in a selected area [17].

The absorption of light from a one-dimensional semiconductor nanostructure can be used to guide the development of highly efficient NW solar cells [18]. Various complications arise when designing solar cells in three dimensions, such as studying the thickness and structural interaction between layers [10]. The structure of SOI solar cells is used to justify the optical performance of antennas [19]. The absorption efficiency is greatly improved when an NW is incorporated into the design of a solar cell [20]. Maximum power (Pmax), voltage (Voc), and light scattering coefficient (Lsc) can change when designing omnidirectional solar cells with a silicon material, although GaAs/Ge solar cells have been modeled in both proton and electron environments [21].

Unlike NWs, the use of nanofluids explains the passage of energy from one port to another, specifies absorption and scattering parameters, and improves the interaction between nanoparticles [22]. These solar cells are used to achieve high efficiency [23] due to the electric field interaction that occurs between them and the electric charge when it passes through space or an electrical conductor. In [24], the electric field and electrical parameters of a stacked model design of GaAs/Ge solar cells were examined in MATLAB under ordinary settings. In [25], numerical FDTD software was used to investigate the optical and electrical properties of different NW diameters, achieving a maximum absorptance of 94% in a wavelength range of 320-455 nm, while increasing the wavelength range the absorptance efficiency decreased. In [26], III-V and II-VI semiconducting materials were integrated to investigate the optoelectronic device physics simulations of GaAs NW solar cells, including recombination models such as heterojunction solar cells, and the optimal design for high efficiency was discussed. In [27], optoelectronic simulations of GaAs NW solar cells showed that efficiency can be improved by optimizing the emitter thickness and extending the intrinsic region. In [28], III-V semiconductor nanomaterials were found to have high electron mobility, a tunable optical bandgap, and suitable optical and electrical properties for photodetection over a broad spectrum range, from deep ultraviolet to THz. In [29], it was shown that the electric field of a GaAs solar cell decreases with increasing incident light intensity due to the PV effect. In [30], the optical properties of III-V semiconductor nanomaterials and their potential for all-optical switching applications were analyzed. In [31], a method for manufacturing tandem solar cells was described using crystalline silicon substrates.

III. SIMULATION METHODOLOGY

Simulations of optical components were carried out using CST's commercial 3D FDTD software. GaAs nanowires were prepared with a diameter (D) ranging from 50 to 200 nm, while their lengths (L) and the length of the Ge bottom cell (P) were maintained at 340 and 50 nm, respectively, and the D/P ratio was maintained constant at 0.5 to determine the best solution. An AM 1.5G light source spanning between 300-2000 nm was used to illuminate the system under study. Periodic boundary conditions were imposed along the z-axis using precisely matched layer methods in the x and y directions.

The absorption coefficient $A(\lambda)$ is the proportion of the incident light at a given wavelength that is retained by the medium it encounters. $T(\lambda)$ is the percentage of a given wavelength of light that passes completely through a certain substance or medium without being absorbed or reflected. $R(\lambda)$ is the percentage of a beam's energy that is reflected from a substance or medium at a certain wavelength. Light at every given wavelength λ is absorbed at a $A(\lambda)$ rate, transmitted at a $T(\lambda)$ rate, and reflected at a $R(\lambda)$ rate. The values of reflectance $R(\lambda)$ and transmission $T(\lambda)$ are determined with the help of frequency domain power monitors. For each given wavelength, $E(\lambda)$ represents the energy of the incident light. The absorbed energy (A) is given by $A(\lambda) \times E(\lambda)$, the transmitted energy (T) is given by $T(\lambda) \times E(\lambda)$, and the reflected energy (R) is given by $R(\lambda) \times E(\lambda)$. As the energy of incident light is conserved,

the sum of the energy absorbed, transmitted, and reflected must equal the energy of the incident light:

$$T(\lambda) \times E(\lambda) + A(\lambda) \times E(\lambda) + R(\lambda) \times E(\lambda) = E(\lambda) \quad (1)$$

$$T(\lambda) + A(\lambda) + R(\lambda) = 1 \quad (2)$$

For a system in which light interacts with a material or medium, the law of energy conservation is represented by (2). These parameters were used to simulate the optical properties of a single GaAs NW on a Ge bottom cell with a 0.5 D/P ratio.

IV. DESIGNING

Figure 1 shows the simulated optical wavefront for an irradiated by sunlight single GaAs NW placed atop a Ge bottom cell.

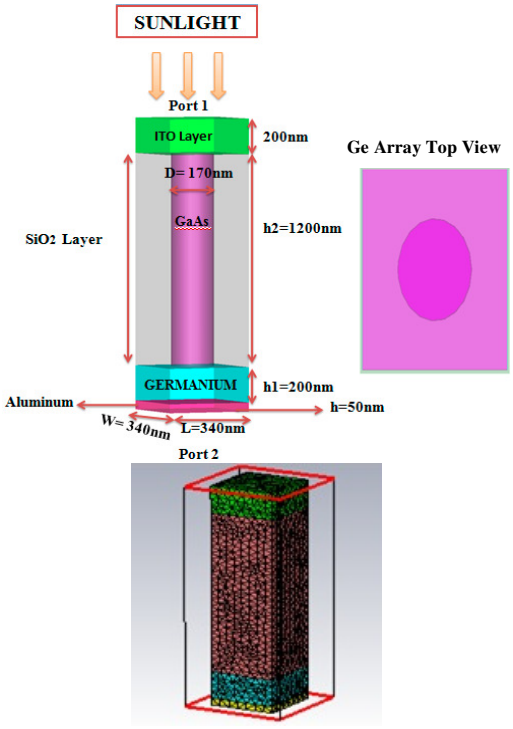

Fig. 1. Top: solar cell top, vertical junction view. Bottom: mesh view.

A boundary condition for the simulating medium was implemented to account for additional loose media on all sides of the simulation zone when modeling a GaAs NW solar cell. As a result, there is no reflection at the interfaces and the inherent impedance matches. GaAs NW and Ge subcell surfaces attenuate electromagnetic fields during propagation inside the media. Measurements of absorption, reflectance, and transmission were taken once the nanowire diameter was optimized for maximum performance.

V. RESULTS AND DISCUSSIONS

Figure 2 shows the transmission, reflection, and absorption spectra of a 170 nm-diameter axial GaAs NW. As the wavelength increases, the strong extinction coefficient of GaAs and the wide bandgap difference between the GaAs NW and the Ge bottom cell cause the peak absorptance (near unity) to fall (λ > 800 nm). A rise in refraction losses is responsible for the drop in absorption spectra between 1000 and 1500 nm. A material having a bandgap between GaAs and Ge can be used to reduce this loss. At an increase in transparency of over 1000 nm, the NW and bottom-cell systems disappear from view. Impedance spectroscopy is used to study the kinetics and energetic processes that govern device performance in both inorganic and organic solar cells. It is also a valuable tool for examining bulk and interfacial electrical properties that cannot be studied under present experimental circumstances. In this technique, a bias voltage is used in conjunction with a tiny sinusoidal voltage. By fitting data from a measurement of an electrical impedance to a circuit model, insight can be gained into the resistance and capacitance of individual cells.

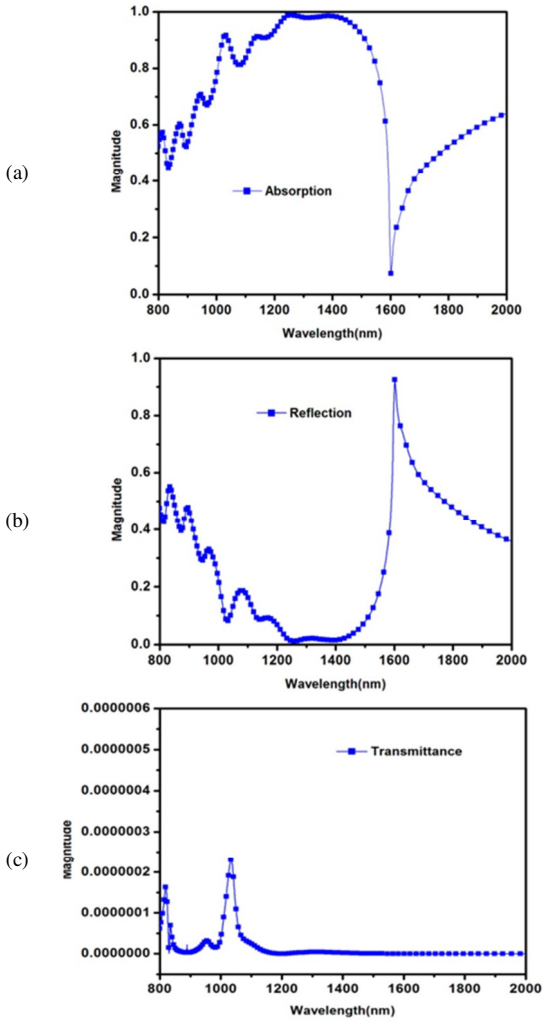

Fig. 2. (a) Absorptance, (b) reflectance, and (c) transmittance of the GaAs NW vertical junction solar cell.

Now, the discussion is on the different field types present in solar cells. One type of field is an electric field (E-field). Solar cells are capable of converting sunlight into electricity. The E-field within a solar cell is an important factor in its operation. As photons strike a solar cell, they excite electrons and cause

them to travel from the valence band to the conduction band, producing an electrical current. The electric field within the solar cell helps to separate the excited electrons from their positively charged counterparts called holes and move them in the right direction to generate electricity. A p-n junction generates the E-field in a solar cell. The solar cell consists of two distinct materials with varying electrical characteristics in this region. The junction creates an E-field that points from the p-type material to the n-type material, and this field helps to separate the excited electrons and holes. In general, the electric field in a solar cell plays a crucial role in its ability to generate electricity from sunlight. Figures 4, 5, and 6 represent the E-field for different port wavelengths of 0.5, 1.35, and 2nm, respectively, and the field passes from Port 1 to Port 2 of the GaAs NW solar cell.

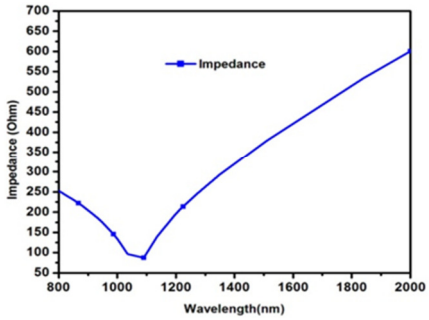

Fig. 3. Impedance of the vertical junction GaAs NW solar cell.

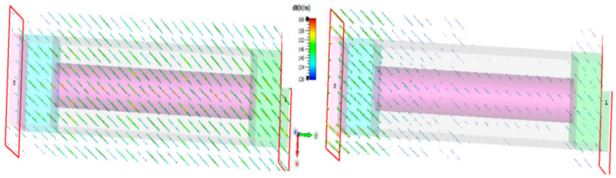

Fig. 4. E-field of the GaAs NW solar cell with a wavelength of 0.5nm from Port 1 to Port 2.

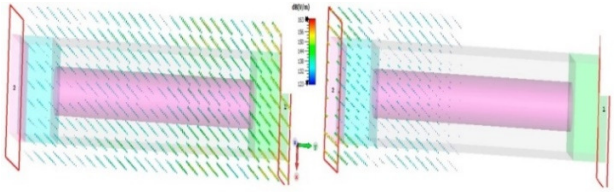

Fig. 5. E-field of the GaAs NW solar cell with a wavelength of 1.35nm from Port 1 to Port 2.

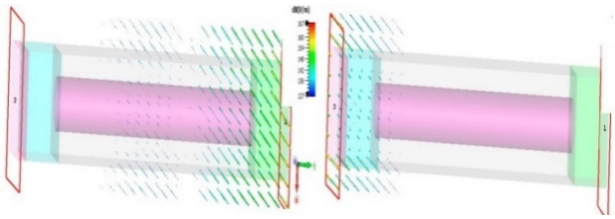

Fig. 6. E-field of the GaAs NW solar cell with a wavelength of 2nm from Port 1 to Port 2.

The magnetic field (H-field) is not directly involved in the operation of solar cells. Instead, solar cells rely on the E-field to generate electricity. The movement of charged particles, such as electrons and holes, within the semiconductor material of the solar cell is what generates the E-field. However, magnetic fields can have an impact on solar cells. Magnetic fields can induce an electric current in a conductor such as the wiring and metal components of a solar cell. This current, called an eddy current, can cause loss and heat within the solar cell, reducing its efficiency. As a result, while constructing and installing solar cells, it is critical to consider the magnetic field environment, particularly in areas with large magnetic fields, such as near power lines or electrical equipment. Figures 7, 8, and 9 represent the H-field for port wavelengths 0.5, 1.35, and 2 nm, respectively, and the field passes from Port 1 to Port 2 of the GaAs NW solar cell. At port wavelength 1.35 nm, the E-field and the H-field operate effectively on the assumed dimensions.

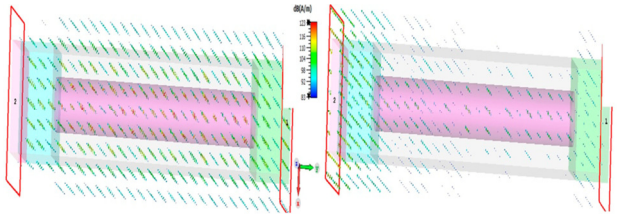

Fig. 7. H-Field of the GaAs NW solar cell with a wavelength of 0.5nm from Port 1 to Port 2.

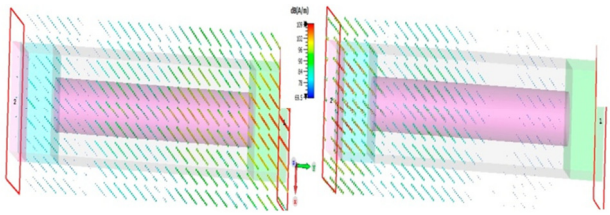

Fig. 8. H-Field of the GaAs NW solar cell with a wavelength of 1.35nm from Port 1 to Port 2.

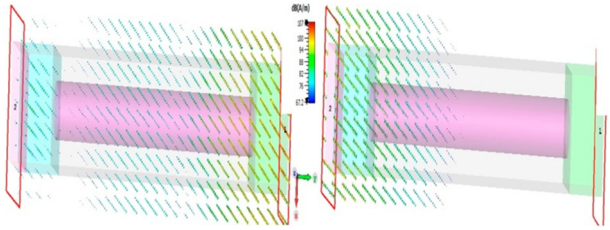

Fig. 9. H-Field of the GaAs NW solar cell with a wavelength of 2nm from Port 1 to Port 2.

Table I shows the percentage of absorptance and reflectance with different radii of NW within the range of λ = 1000-1800 nm. Figures 10 and 11 show the absorption and reflection for different radii of GaAs NW. It can be noted that there is increased absorbance and reduced reflection at shorter wavelengths of 1000-1800 nm.

TABLE I. ABSORPTANCE AND REFLECTANCE FOR DIFFERENT NANOWIRE RADIUS

Radius (nm)	λ = 1000-1800 nm	
	Maximum Absorptance (%)	Minimum Reflectance (%)
85	99	0.9
90	94	5.8
95	91	8.7
100	87	11.5

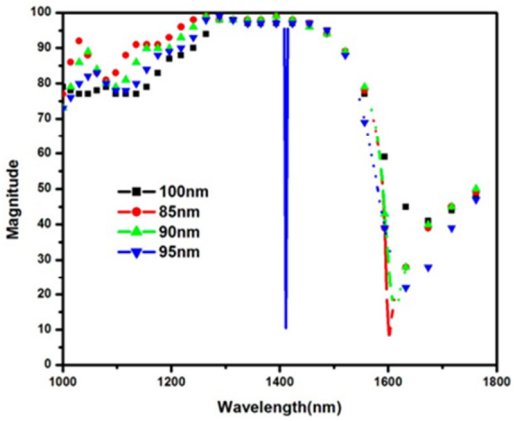

Fig. 10. Absorption spectra for different GaAs NW radii.

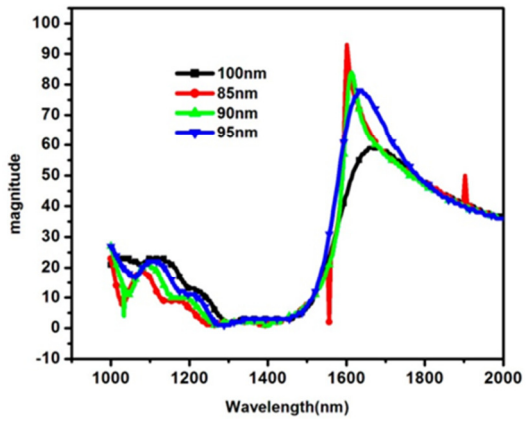

Fig. 11. Reflectance results for different GaAs NW radii.

Depending on the radius of the NW and how much light is reflected or transmitted, a certain mode will resonate, governing its light absorption. Understanding the relationships between NWs' geometrical characteristics and their various light-absorbing mechanisms is crucial for achieving maximum light absorption. In this process, a maximum absorptance of 99% was obtained at a 1243-1397 nm wavelength with an NW radius of 85 nm.

VI. CONCLUSION

This study used the 3D FDTD approach implemented in CST software to conduct a comprehensive analysis of GaAs NW with Ge bottom-cell solar cells to optimize their geometrical characteristics and study their solar cell performance in E-Field and H-Field at varying port wavelengths. The electrical properties of a GaAs NW cylinder had a maximum absorptance of 99% in the wavelength range of 1243-1397 nm for a radius of 85 nm. Its absorptance was 94%, 91%, and 87% when the radius was 90, 95, and 100 nm. Therefore, as the radius of the GaAs nanowire cylinder increases, the absorptance percentage decreases. The electric field and magnetic field of a single junction GaAs NW - Ge solar cell were determined with different port wavelengths of 0.5, 1.35, and 2 nm. It was observed that at 1.35nm, the E-field and H-field were conducted and provided better optical and electrical properties.

REFERENCES

[1] I. Mora-Seró, G. Garcia-Belmonte, P. P. Boix, M. A. Vázquez, and J. Bisquert, "Impedance spectroscopy characterisation of highly efficient silicon solar cells under different light illumination intensities," *Energy & Environmental Science*, vol. 2, no. 6, pp. 678–686, 2009, https://doi.org/10.1039/B812468J.

[2] R. Anil Kumar, M. S. Suresh, and J. Nagaraju, "Measurement and comparison of AC parameters of silicon (BSR and BSFR) and gallium arsenide (GaAs/Ge) solar cells used in space applications," *Solar Energy Materials and Solar Cells*, vol. 60, no. 2, pp. 155–166, Jan. 2000, https://doi.org/10.1016/S0927-0248(99)00080-X.

[3] G. Garcia-Belmonte, P. P. Boix, J. Bisquert, M. Sessolo, and H. J. Bolink, "Simultaneous determination of carrier lifetime and electron density-of-states in P3HT:PCBM organic solar cells under illumination by impedance spectroscopy," *Solar Energy Materials and Solar Cells*, vol. 94, no. 2, pp. 366–375, Feb. 2010, https://doi.org/10.1016/j.solmat.2009.10.015.

[4] T. Ripolles-Sanchis, A. Guerrero, J. Bisquert, and G. Garcia-Belmonte, "Diffusion-Recombination Determines Collected Current and Voltage in Polymer:Fullerene Solar Cells," *The Journal of Physical Chemistry C*, vol. 116, no. 32, pp. 16925–16933, Aug. 2012, https://doi.org/10.1021/jp305941f.

[5] D. V. Prashant, D. P. Samajdar, and D. Sharma, "Optical simulation and geometrical optimization of P3HT/GaAs nanowire hybrid solar cells for maximal photocurrent generation via enhanced light absorption," *Solar Energy*, vol. 194, pp. 848–855, Dec. 2019, https://doi.org/10.1016/j.solener.2019.11.027.

[6] S. P. Tobin, S. M. Vernon, C. Bajgar, V. E. Haven, L. M. Geoffroy, and D. R. Lillington, "High-efficiency GaAs/Ge monolithic tandem solar cells," *IEEE Electron Device Letters*, vol. 9, no. 5, pp. 256–258, Feb. 1988, https://doi.org/10.1109/55.708.

[7] Z. Li, H. H. Tan, C. Jagadish, and L. Fu, "III–V Semiconductor Single Nanowire Solar Cells: A Review," *Advanced Materials Technologies*, vol. 3, no. 9, 2018, Art. no. 1800005, https://doi.org/10.1002/admt.201800005.

[8] E. C. Garnett, M. L. Brongersma, Y. Cui, and M. D. McGehee, "Nanowire Solar Cells," *Annual Review of Materials Research*, vol. 41, no. 1, pp. 269–295, 2011, https://doi.org/10.1146/annurev-matsci-062910-100434.

[9] Sachchidanand and D. P. Samajdar, "Light-trapping strategy for PEDOT:PSS/c-Si nanopyramid based hybrid solar cells embedded with metallic nanoparticles," *Solar Energy*, vol. 190, pp. 278–285, Sep. 2019, https://doi.org/10.1016/j.solener.2019.08.023.

[10] J.-P. Berenger, "A perfectly matched layer for the absorption of electromagnetic waves," *Journal of Computational Physics*, vol. 114, no. 2, pp. 185–200, Oct. 1994, https://doi.org/10.1006/jcph.1994.1159.

[11] L. Cao *et al.*, "Semiconductor Nanowire Optical Antenna Solar Absorbers," *Nano Letters*, vol. 10, no. 2, pp. 439–445, Feb. 2010, https://doi.org/10.1021/nl9036627.

[12] J. Z. Zhang, Optical Properties And Spectroscopy Of Nanomaterials. Singapore: World Scientific, 2009.

[13] J. Wong-Leung *et al.*, "Engineering III–V Semiconductor Nanowires for Device Applications," *Advanced Materials*, vol. 32, no. 18, 2020, Art. no. 1904359, https://doi.org/10.1002/adma.201904359.

[14] Z. Gu, P. Prete, N. Lovergine, and B. Nabet, "On optical properties of GaAs and GaAs/AlGaAs core-shell periodic nanowire arrays," *Journal*

of Applied Physics, vol. 109, no. 6, Mar. 2011, Art. no. 064314, https://doi.org/10.1063/1.3555096.

[15] L. Wen, Z. Zhao, X. Li, Y. Shen, H. Guo, and Y. Wang, "Theoretical analysis and modeling of light trapping in high efficicency GaAs nanowire array solar cells," *Applied Physics Letters*, vol. 99, no. 14, Oct. 2011, Art. no. 143116, https://doi.org/10.1063/1.3647847.

[16] P. A. Iles, Y. C. M. Yeh, F. H. Ho, C. L. Chu, and C. Cheng, "High-efficiency (>20% AM0) GaAs solar cells grown on inactive-Ge substrates," *IEEE Electron Device Letters*, vol. 11, no. 4, pp. 140–142, Apr. 1990, https://doi.org/10.1109/55.61775.

[17] Y. Minami, A. Yoshida, J. Motohisa, and K. Tomioka, "Growth and characterization of GaAs nanowires on Ge(1 1 1) substrates by selective-area MOVPE," *Journal of Crystal Growth*, vol. 506, pp. 135–139, Jan. 2019, https://doi.org/10.1016/j.jcrysgro.2018.10.009.

[18] T. J. Kempa, R. W. Day, S.-K. Kim, H.-G. Park, and C. M. Lieber, "Semiconductor nanowires: a platform for exploring limits and concepts for nano-enabled solar cells," *Energy & Environmental Science*, vol. 6, no. 3, pp. 719–733, Feb. 2013, https://doi.org/10.1039/C3EE24182C.

[19] E. S. Barnard, R. A. Pala, and M. L. Brongersma, "Photocurrent mapping of near-field optical antenna resonances," *Nature Nanotechnology*, vol. 6, no. 9, pp. 588–593, Sep. 2011, https://doi.org/10.1038/nnano.2011.131.

[20] J. Kupec, R. L. Stoop, and B. Witzigmann, "Light absorption and emission in nanowire array solar cells," *Optics Express*, vol. 18, no. 26, pp. 27589–27605, Dec. 2010, https://doi.org/10.1364/OE.18.027589.

[21] J. Kupec, R. L. Stoop, and B. Witzigmann, "Light absorption and emission in nanowire array solar cells," *Optics Express*, vol. 18, no. 26, pp. 27589–27605, Dec. 2010, https://doi.org/10.1364/OE.18.027589.

[22] H. A. Fakhim, "An Investigation of the Effect of Different Nanofluids in a Solar Collector," *Engineering, Technology & Applied Science Research*, vol. 7, no. 4, pp. 1741–1745, Aug. 2017, https://doi.org/10.48084/etasr.1283.

[23] M. E. Bendib and A. Mekias, "Solar Panel and Wireless Power Transmission System as a Smart Grid for Electric Vehicles," *Engineering, Technology & Applied Science Research*, vol. 10, no. 3, pp. 5683–5688, Jun. 2020, https://doi.org/10.48084/etasr.3473.

[24] S. E. T. Moghaddam and S. M. Kankanani, "Numerical Simulation of a Mechanically Stacked GaAs/Ge Solar Cell," *Engineering, Technology & Applied Science Research*, vol. 7, no. 3, pp. 1611–1614, Jun. 2017, https://doi.org/10.48084/etasr.935.

[25] L. M. Ali and F. A. Abed, "Investigation of opto-electric characterization of GaAs/In0.2Ga0.8As nanowire solar cell," *Materials Research Express*, vol. 6, no. 4, Jan. 2019, Art. no. 045062, https://doi.org/10.1088/2053-1591/aaffee.

[26] P. R. Jahelka and H. A. Atwater, "Non-Epitaxial GaAs Heterojunction Nanowire Solar Cells (PVSC)," in *2019 IEEE 46th Photovoltaic Specialists Conference (PVSC)*, Chicago, IL, USA, Jun. 2019, vol. 2, pp. 1–8, https://doi.org/10.1109/PVSC40753.2019.9198966.

[27] A. H. Trojnar, C. E. Valdivia, R. R. LaPierre, K. Hinzer, and J. J. Krich, "Optimizations of GaAs Nanowire Solar Cells," *IEEE Journal of Photovoltaics*, vol. 6, no. 6, pp. 1494–1501, Aug. 2016, https://doi.org/10.1109/JPHOTOV.2016.2600339.

[28] K. Sarkar, P. Devi, K.-H. Kim, and P. Kumar, "III-V nanowire-based ultraviolet to terahertz photodetectors: Device strategies, recent developments, and future possibilities," *TrAC Trends in Analytical Chemistry*, vol. 130, Sep. 2020, Art. no. 115989, https://doi.org/10.1016/j.trac.2020.115989.

[29] S. SaeidNahaie *et al.*, "Investigation of the incident light intensity effect on the internal electric fields of GaAs single junction solar cell using bright electroreflectance spectroscopy," *Current Applied Physics*, vol. 20, no. 1, pp. 145–149, Jan. 2020, https://doi.org/10.1016/j.cap.2019.10.006.

[30] V. Snigirev, A. Shorokhov, D. Gulkin, V. Bessonov, I. Soboleva, and A. Fedyanin, "Ultrafast all-optical switching in III-V semiconductor resonant nanostructures," in *2019 Conference on Lasers and Electro-Optics Europe and European Quantum Electronics Conference (2019)*, Munich, Germany, Jun. 2019.

[31] Y. J. Lee, S. KIM, S.-W. Ahn, and J.-W. Chung, "Tandem solar cell manufacturing method," US11515443B2, Nov. 29, 2022.